

A New Approach to HF Channel Modeling and Simulation Part III: Transfer Function

L.E. Vogler
J.A. Hoffmeyer



U.S. DEPARTMENT OF COMMERCE
Barbara Hackman Franklin, Secretary

Thomas J. Sugrue, Acting Assistant Secretary
for Communications and Information

March 1992

CONTENTS

	Page
LIST OF FIGURES.....	iv
ABSTRACT.....	1
1. INTRODUCTION.....	1
2. MODEL TRANSFER FUNCTION.....	3
3. COMPARISONS OF MODEL AND MEASUREMENTS.....	12
4. SUMMARY.....	15
5. ACKNOWLEDGMENTS.....	16
6. REFERENCES.....	30
APPENDIX.....	32

LIST OF FIGURES

	Page
Figure 1.	Delay amplitude shape factor.....17
Figure 2.	Scattering function at 3.3 MHz; minimally dispersive channel.....18
Figure 3.	Scattering function at 5.3 MHz; minimally dispersive channel.....19
Figure 4.	Simulated scattering function for Figure 2 (3.3 MHz).....20
Figure 5.	Simulated scattering function for Figure 3 (5.3 MHz).....21
Figure 6.	Scattering function at 3.3 MHz; overhead ionospheric trough.....22
Figure 7.	Scattering function at 5.3 MHz; overhead ionospheric trough.....23
Figure 8.	Simulated scattering function for Figure 6 (3.3 MHz).....24
Figure 9.	Simulated scattering function for Figure 7 (5.3 MHz).....25
Figure 10.	Scattering function at 2.8 MHz; isolated magnetic disturbance.....26
Figure 11.	Scattering function at 3.8 MHz; isolated magnetic disturbance.....27
Figure 12.	Simulated scattering function for Figure 10 (2.8 MHz).....28
Figure 13.	Simulated scattering function for Figure 11 (3.8 MHz).....29

A NEW APPROACH TO HF CHANNEL MODELING AND SIMULATION

PART III: TRANSFER FUNCTION

L.E. Vogler and J.A. Hoffmeyer*

This is the third in a series of reports which describe a new and unique approach for modeling either narrowband or wideband high frequency (HF) channels. Although narrowband models of the HF channel have existed for many years, they are applicable to only a limited set of actual narrowband propagation conditions. The need for an HF channel model that is valid for both narrow and wide bandwidths over a more extensive range of propagation conditions motivated the research documented in this series of reports.

An explicit expression for the channel transfer function incorporating a random time-varying generator is derived and its relation to the impulse response and scattering function is discussed. Comparisons with measured data indicate the process is best modeled as a sequence of random variables with an exponential autocorrelation function; this leads to a scattering function having a Lorentzian shape. A brief discussion of a Gaussian random variable generator is also included. Comparisons of scattering functions from the model and from measurements on a near-vertical incidence auroral path for a wide range of spread-F conditions are shown.

Key Words: channel transfer function; HF channel models; HF propagation; scattering functions; spread spectrum communications; wideband HF

1. INTRODUCTION

A new model to simulate the sky-wave propagation conditions that occur in a high frequency (HF) communication link has been under development at ITS during recent years (Hoffmeyer and Nesenbergs, 1987; Vogler et al., 1988; Hoffmeyer and Vogler, 1990). Older models have been restricted to limited narrowband applications and are inadequate for the investigation of wideband

* The authors are with the Institute for Telecommunication Sciences, National Telecommunication and Information Administration, U. S. Department of Commerce, Boulder, CO 80303-3328

spread spectrum techniques. The recently developed approach has been discussed in two previously published reports (Vogler and Hoffmeyer, 1988; Vogler and Hoffmeyer, 1990) that describe the deterministic and stochastic aspects of the model. This model is currently being implemented in a hardware HF simulation System that will be useful for testing all types of HF systems-- conventional narrowband, frequency hopping, and direct sequence spread spectrum.

The HF channel simulation model assumes four ionospheric input parameters that can be obtained either from observations or from some reliable ionospheric prediction model: penetration frequency (f_p), layer height (h_o), layer thickness (σ), and an estimate of received signal attenuation (A). Typically, ionospheric prediction models are used to provide monthly median and 90th percentile values of parameters that can be used to determine propagation characteristics including the received signal level. These parameters are predicted through the use of ionospheric data bases that are functions of geographic location, sunspot number (SSN), time of day, and month. Used in conjunction with models of the noise environments and characteristics of the transmitting and receiving antennas, these parameters form the basis for HF link performance calculations that permit the evaluation of predicted signal-to-noise ratios at any point on the earth's surface.

The channel simulation model, on the other hand, is a model that provides an emulation of all aspects of the time-varying channel on the transmitted signal --not just the effect of the channel on the received signal which is usually calculated by most link prediction programs. The present channel simulation model includes the effects of Doppler shift, Doppler spread, group time delay dispersion, and delay spread. The group time delay dispersion is caused by the reflection of different frequency components of the transmitted signal at different ionospheric layer heights. Additional delay spread or smearing of the transmitted signal in the time domain is caused by irregularities in the ionosphere. This effect is particularly noticeable on polar and

trans-auroral paths, but can also be seen frequently on mid-latitude paths when spread-F conditions occur. A HF simulation model attempts to model more effects of the time-varying ionospheric channel than is provided by typical link prediction modeling programs. Accurate prediction of digital HF radio performance requires the use of all of the parameters mentioned above.

In the following pages the derivation of the transfer function that is used in the ITS simulation model is given. The introduction of random variation in the transmitted signal is described and generation of the random process is explained. Comparisons are then shown of the simulation model with the results of actual measurements over an auroral path.

2. MODEL TRANSFER FUNCTION

The ionospheric channel pulse response $y(\tau, t)$ is expressible as the inverse Fourier transform of the product of the source pulse frequency response $\tilde{S}_T(\bar{f})$ and the channel transfer function $H(\bar{f}, t)$:

$$y(\tau, t) = \int_{-\infty}^{+\infty} \sum_{n=1}^N H_n(\bar{f}, t) \tilde{S}_T(\bar{f}) e^{i2\pi\bar{f}\tau} d\bar{f}, \quad (1)$$

where in terms of the radio frequency f and carrier frequency f_c , $\bar{f} = f - f_c$. The delay time τ is associated with the distance separation between transmitter and receiver and also with the dispersive properties of the ionosphere, whereas the time t is the time over which the structural and compositional characteristics of the ionosphere vary. The index n refers to a particular layer-mode (e.g., the ordinary wave, low-ray, one-hop F layer component) and, depending on the propagation path, may range from one to eight or more. To simplify notation, the n subscript will be dropped in the following discussion with the understanding that the equations are applicable to any of the several layer-modes.

The mathematical form that has been assumed to represent the transfer function was chosen in order to simulate the variety of delay time and Doppler frequency characteristics that are seen in measured data. A justification for the analytical forms lies in the fact that the resulting delay and Doppler shapes appear to compare well with actual measurements. There are six physical quantities that determine the simulated shapes and that are assumed as basic input:

Time Delay, τ

- τ_U = upper or maximum value of τ
- τ_L = lower or minimum value of τ
- A = peak amplitude at $\tau=\tau_c$

Doppler Frequency, f_D

- f_s = Doppler shift at $\tau=\tau_c$
- f_{sL} = Doppler shift at $\tau=\tau_L$
- σ_D = half-width of Doppler spread at $\tau=\tau_c$

The delay time τ_c , associated with the carrier frequency f_c , is discussed later on. Also, it is often more convenient to input the total and partial delay spreads, $\sigma_T=\tau_U-\tau_L$ and $\sigma_c=\tau_c-\tau_L$, rather than the upper and lower τ values. In any case, the six input values normally will be obtained from empirically determined ranges and distributions of the above quantities.

The manner in which the model transfer function was developed is outlined in the following paragraphs. First, certain analytic forms were assumed for the scattering functions $S(\tau, f_D)$. These forms were arrived at by studying many different measured scattering functions to determine the key parameters and shapes that would best characterize their dependence on delay time and Doppler frequency. The parameters chosen were the input quantities given above; explicit expressions for the shapes will be given later.

Next, it can be shown that the scattering function is the Fourier transform of the autocorrelation function of the received impulse response as a function of time t (Proakis, 1983; pp. 461-463). Thus, if t_l denotes the time lag, the autocorrelation function $R(\tau, t_l)$ can be found from

$$R(\tau, t_l) = \int_{-\infty}^{+\infty} S(\tau, f_D) \exp(i2\pi f_D t_l) df_D, \quad (2)$$

where $R(\tau, t_l)$ is also expressed as

$$R(\tau, t_l) = C_o \int_{-\infty}^{+\infty} h^*(\tau, t) h(\tau, t+t_l) dt, \quad (3)$$

with $h(\tau, t)$ representing the received signal in time t , C_o is a normalizing constant, and the asterisk is the usual symbol for complex conjugation. Notice that the variation over t in (3) is for a fixed delay time τ .

The next step in the development of the model transfer function is to determine the received time signal $h(\tau, t)$ through the relationship given in (3). The signal contains the effects of both the delay time and the normal time, but it is the delay that is associated with radio frequency and, consequently, leads to the transfer function using a Fourier transform:

$$H(\bar{f}, t) = \int_{-\infty}^{+\infty} h(\tau, t) \exp(-i2\pi \bar{f} \tau) d\tau, \quad (4)$$

where $h(\tau, t)$ now represents the layer-mode impulse response $h_n(\tau, t)$. In the simulation of a particular communication system, of course, the actual frequency response of the source would be used in conjunction with $H_n(\bar{f}, t)$ as indicated in (1).

The procedure described above results in the following nonrandom, analytical expression for the model transfer function:

$$\begin{aligned}
 H(\bar{f}, t) &= C e^{-\gamma_0 t} [G(\bar{f}, t) e^{i2\pi\bar{f}\tau_i}]^{-1}, & (5) \\
 C &= e^{i2\pi\phi_0} \sqrt{A} \sigma_i \{e^{\alpha/2} \Gamma(1+\alpha/2) / (\alpha/2)^{1+\alpha/2}\}, \\
 G(\bar{f}, t) &= \{i4\pi(\sigma_i/\alpha)(\bar{f}-bt)+1\}^{1+\alpha/2}, \\
 \gamma_0 &= \zeta - i2\pi(f_s - b\sigma_i), \quad b = (f_s - f_{sL}) / (\tau_c - \tau_L), \quad \sigma_i = \tau_c - \tau_i,
 \end{aligned}$$

and $\Gamma(\cdot)$ denotes the Gamma function (Abramowitz and Stegun, 1964; p. 255). The phase term ϕ_0 and amplitude A are assumed constant (for a given layer-mode) in the present version of the model although either could be made to vary in a more generalized version. The parameters α and τ_i are functions of the delay spread and received signal threshold, and their computation is described in the Appendix.

The quantity τ_c denotes the delay time associated with the frequency component at f_c and is evaluated from an expression derived using a sech^2 electron density profile (Vogler and Hoffmeyer, 1988):

$$\begin{aligned}
 f_c &= f_p \left[\{1 + (D/2\bar{h})^2\} / \{1 + e^{(h_0 - \bar{h})/\sigma}\} \right]^{1/2}, \\
 \bar{h} &= \{(c\tau_c/2)^2 - (D/2)^2\}^{1/2}, & (6)
 \end{aligned}$$

where h_0 , σ , and f_p represent, respectively, the height at which maximum density occurs, thickness scale factor, and penetration frequency of the ionospheric layer; D is the path distance and c is the speed of light.

The shape of the Doppler spread is determined by ζ , which in turn is defined according to whether a Gaussian- or a Lorentzian-Doppler shape is desired. In terms of the Doppler spread half-width σ_D and the received signal threshold A_{fl} .

$$\text{Gaussian: } \zeta = \pi \sigma_f^2 t, \quad \sigma_f = \sigma_D \{(-\ln s_v) / \pi\}^{-1/2}, \quad (7a)$$

$$\text{Lorentzian: } \zeta = \sigma_f, \quad \sigma_f = 2\pi \sigma_D s_v \{(1-s_v^2)\}^{-1/2}, \quad (7b)$$

where $s_v = A_{f_l}/A$. The question as to which Doppler shape corresponds most nearly to reality can only be answered by comparisons with actual measurements; and it may well be that both shapes are suitable under different ionospheric conditions.

With the model transfer function now defined in (5), it is a straightforward matter to obtain expressions for both the layer-mode impulse response $h(\tau, t)$ and the scattering function $S(\tau, f_D)$. The impulse response is the inverse Fourier transform of $H(\bar{f}, t)$ over \bar{f} :

$$h(\tau, t) = \int_{-\infty}^{+\infty} H(\bar{f}, t) e^{i2\pi\bar{f}\tau} d\bar{f} = e^{i2\pi\theta_0 - \gamma_1 t} \{T(\tau)\}^{1/2}, \quad (8a)$$

$$\text{where } T(\tau) = A e^{\alpha(\ln g + 1 - g)}, \quad g = (\tau - \tau_l) / \sigma_t > 0, \quad (8b)$$

$$\gamma_1 = \zeta - i2\pi f_B, \quad f_B = f_s + b(\tau - \tau_c), \quad (8c)$$

and the transform pair can be found in Campbell and Foster (1948; 524.2, p. 51).

The shape factor $T(\tau)$ determines how the impulse response behaves as a function of delay time τ . A representative sketch of $T(\tau)$ is shown in Figure 1. The maximum always occurs at $\tau = \tau_c$, however the position of the peak along the τ axis can vary (with the restriction that $\sigma_c < \sigma_t/2$). Shapes can be obtained that range from very skewed to almost symmetrical.

The exponential factor γ_1 contains the amplitudes and phase constants that characterize Doppler frequency effects. The inclusion of τ in the imaginary part provides the "slant" phenomenon that is observed so frequently in measured scattering functions (Wagner et al., 1989).

To obtain the scattering function, it is first necessary to find the autocorrelation of $h(\tau, t)$ with respect to τ . For the shapes assumed in the present model (Gaussian and Lorentzian), the t_i dependence of $R(\tau, t_i)$ has the same form as (8a) with t replaced by the lag time t_i ; i.e., from (3).

$$R(\tau, t_i) = C_0 T(\tau) e^{-\gamma_1 t_i}, \quad (9)$$

where ζ in (8c) is given by (7) with $t = t_i$. The scattering function is now obtained from the Fourier transform of (9) over t_i :

$$S_G(\tau, f_D) = \sqrt{T(\tau)} e^{i2\pi\sigma_o} e^{-\pi\{(f_D - f_B)/\sigma_f\}^2}, \quad (\text{Gaus.}) \quad (10a)$$

$$S_L(\tau, f_D) = \sqrt{T(\tau)} e^{i2\pi\sigma_o} \left\{ \frac{\sigma_f}{i2\pi(f_D - f_B) + \sigma_f} \right\}, \quad (\text{Loren.}) \quad (10b)$$

where a factor σ_f has been included for normalization purposes and the transforms can be found in Campbell and Foster (1948; 438, p. 45 and 708.0, p. 84). For pictorial representation, a three-dimensional plot of the scattering function is often shown using $|S(\tau, f_D)|$ versus τ and f_D .

The foregoing discussion of the HF channel simulation model describes a transfer function capable of providing those characteristics of a received signal that are of primary concern to the communication systems engineer, such as delay and Doppler spreads and Doppler shifts. However, the constantly shifting changes in electron density that cause the random variation of received time signals observed in most HF systems have yet to be treated. This aspect of the simulation is accomplished by introducing a random process to replace the analytic variation of signal strength specified by $\exp(-\zeta t)$ in (8). The process must be such that the shifts and spreads characterizing the ionospheric conditions remain after appropriate analysis of the received signal time series.

We start by recognizing that the simulation model should be formulated as a discrete function rather than a continuous one. Thus, the impulse response in (8) is now represented by

$$h(\tau_k, t_m) = e^{i2\pi\phi_0\{T(\tau_k)\}^{1/2}} z(k, m) e^{i\eta(k)t_m}, \quad (11)$$

$$\text{where } \eta(k) = 2\pi\{f_s + b(\tau_k - \tau_c)\}, \quad z(k, m) = x(k, m) + iy(k, m), \quad (12a)$$

$$t_m = t_0 + m\Delta t, \quad \tau_k = \tau_0 + k\Delta\tau, \quad (k, m=0, 1, 2, \dots) \quad (12b)$$

and $x(k, m)$, $y(k, m)$ are independent, random (real) variables that satisfy certain conditions to be discussed. The incremental times Δt , ΔT are constants chosen by the analyst or by the simulator builder, and τ_c is that value of τ corresponding to $\bar{f} = f - f_c = 0$ (see (6)).

One condition that the random variables (rv) should satisfy is that their autocorrelation over t_m tend to the analytical value given by the real part of the exponential in (9) as the total number of sample variables M becomes large. For a fixed value of τ_k and with $C(k)$ denoting the constant factors, the autocorrelation of $h(\tau_k, t_m)$ from (11) and (3) can be written as

$$\begin{aligned} R(\tau_k, t_\ell) &= \frac{C(k)}{M-\ell} \sum_{m=1}^{M-\ell} h^*(\tau_k, t_m) h(\tau_k, t_{m+\ell}) \\ &= \frac{C(k)}{M-\ell} e^{i\eta(k)t_\ell} \sum_{m=1}^{M-\ell} (x_m - iy_m)(x_{m+\ell} + iy_{m+\ell}) \\ &= \frac{C(k)}{M-\ell} e^{i\eta(k)t_\ell} \sum_{m=1}^{M-\ell} (x_m x_{m+\ell} + y_m y_{m+\ell}), \end{aligned} \quad (13)$$

where $\ell = 0, 1, 2, \dots$ and summation over the cross-products of x and y is zero because of their assumed independence. The index k in x and y has been dropped to simplify notation.

A means of generating rv's having an exponential autocorrelation function (leading to the scattering function of (10b)) is described in Naylor et al. (1966; p.120). For sequences

of independent rv's ρ_m and ρ'_m , the exponentially correlated random process can be generated from

$$\begin{aligned} x_m &= \rho_m + (x_{m-1} - \rho_m)\lambda, y_m = \rho'_m + (y_{m-1} - \rho'_m)\lambda, \\ x_o &= (1-\lambda)\rho_o, y_o = (1-\lambda)\rho'_o, \lambda = \exp[-(\Delta t)\sigma_f], \end{aligned} \quad (14)$$

with σ_f given by (7b).

Generating random variables having a Gaussian-shaped autocorrelation function (leading to the scattering function of (10a)) can be accomplished by first taking the Fourier transform of a sequence of independent rv's such as the ρ_m above, then multiplying this output by the filter function $\exp[-2\pi(f_m/\sigma_f)^2]$, and finally taking the inverse Fourier transform of the product resulting from the second step. Notice that this process leads to a restricted set of numbers, whereas the method of (14) produces an open set. Thus, the transforms should be done over as large a sample size as storage restrictions will allow.

A second condition for the rv's concerns fading characteristics. In order that the long-term fading statistics of the signal follow the usual Rayleigh distribution, ρ and ρ' are chosen to be independent, zero-mean Gaussian processes with a common variance: this is equivalent to the bivariate Gaussian hypothesis assumed in the Watterson model (Watterson et al., 1970).

As mentioned previously, the above equations defining the various quantities of the model have referred to only one layer-mode. For each of the N layer-modes a set of input parameters is entered, and the total impulse response is given by

$$h(\tau_k, t_m) = \sum_{n=1}^N h_n(\tau_k, t_m). \quad (15)$$

The model transfer function with the inclusion of the random process then is obtained by a discrete Fourier transform over the τ variable:

$$H(\kappa/K\Delta\tau, t_m) = \sum_{k=0}^{K-1} h(k\Delta\tau, t_m) \exp(-i2\pi\kappa k/K), (\kappa=0, 1, \dots, K-1) \quad (16)$$

where the impulse responses h_n are computed using (11).

Notice that the conditions imposed on the random process denoted by $z(k, m)$ in (12a) determine the shape of Doppler spread in the simulation model. A Fourier transform of a purely random process produces a spectrum that has no shape. The Doppler spread and Doppler shape arise from a Fourier transform of the autocorrelation of the random signal.

3. COMPARISONS OF MODEL AND MEASUREMENTS

A propagation measurement program using the Naval Research Laboratory wideband HF prober in the auroral region was undertaken recently over a near-vertical 80 km east-west path near Fairbanks, Alaska (Wagner and Goldstein, 1991). The measurements were made during May of 1988 and covered a variety of ionospheric conditions ranging from quiet and stable to intense spread-F. The data is described in terms of the scattering function and, thus, can be compared directly with the simulation model. The input parameters to the model for the different figures are given in Table 1.

Table 1. Parameters Used in the Simulations

	D (km)	f_c (MHz)	f_p (MHz)	σ (km)	h_o (km)	A	σ_r (μs)	σ_c (μs)	σ_D (Hz)	f_s (Hz)	f_{sL} (Hz)
Fig. 4	88	3.3	6.00	26	228	1 0	22 0	10.7 0	0.1 0	-0.05 0	-0.05 0
Fig. 5	88	5.3	7.07	20	225	0.8 0	80 0	39.2 0	0.12 0	-0.05 0	-0.05 0
			5.56	26	228	1 0	240 0	117.8 0	0.15 0	-0.05 0	-0.05 0
Fig. 8	88	3.3	6.48	40	205	1 0	350 0	170 0	2.4 0	-0.8 0	-0.8 0
			6.59	30	240	1 0	400 0	195 0	1.4 0	0.4 0	0.4 0
Fig. 9	88	5.3	6.59	30	240	1 0	1600 0	300 0	4.0 0	-0.65 0	-0.8 0
Fig. 12	88	2.8	5.87	30	240	0.25 0	350 0	170 0	5.0 0	1.1 0	0.8 0
Fig. 13	88	3.8	6.57	50	150	1 0	300 0	147.6 0	8.0 0	0 0	0 0
			5.87	30	240	1 0	1400 0	300 0	9.0 0	-1.6 0	-2.0 0

A relatively benign condition is first shown in Figures 2 and 3 for two different carrier frequencies, 3.3 and 5.3 MHz. The higher frequency (Figure 3), showing both the O- and X-modes, has a larger delay spread because it is nearer the critical frequency where more dispersion is expected. The two plots in each figure show a three-dimensional representation of the scattering function on the right and a contour plot (looking directly down) on the left.

The corresponding simulations are shown in Figures 4 and 5. The difference in delay scales between the model and measurements arises from the fact that the measurements are plotted relative to an arbitrary delay value, whereas the model shows the simulated delay time between transmitter and receiver. The quiet ionospheric conditions were simulated by allowing the random process z in (11) to change less frequently than during spread-F conditions. The result is a scatter function that looks more deterministic. Because of the randomness, it is not possible to duplicate exactly the measured plots; however, the model appears to simulate the main features reasonably well.

Another set of measurements were made during moderate spread-F conditions. Scattering functions for this case are shown in Figures 6 and 7 for the two frequencies 3.3 and 5.3 MHz. The plot shown furthest to the right is the actual unsmoothed scatter function obtained directly from the data. In the other two representations, a 4-point triangular smoothing has been applied to the unsmoothed version. Without the smoothing, the contour plot would look chaotic; on the other hand the contour plot does not give a very accurate picture of the true scatter function for the 5.3 MHz data.

Simulations of the moderate spread-F results are shown in Figures 8 and 9. The unsmoothed, smoothed, and contour representations are quite similar to the 3.3 MHz measured versions. The contour levels differ because of software plotting package differences; however, the lowest contours in each plot are approximately equivalent even though the labeling is not the same.

The more pronounced scattering of the spread-F increases both the delay and Doppler spreads, and the model reproduces this effect by adjusting the input parameters as listed in Table 1. The model and measurement plots are quite similar except in the case of the contours for 5.3 MHz.

An example of intense spread-F conditions is shown in the measured data of Figures 10 and 11, with the corresponding simulations in Figures 12 and 13. The measurements were taken at 2.8 and 3.8 MHz, and the returns at the lower frequency were becoming so faint that a relatively short delay spread was measured although the Doppler spread is larger than before. The full extent of delay and Doppler spread associated with intense spread-F is displayed in Figure 11. The two parts of the return are most likely from different regions of the ionosphere, but the model is able to simulate the result (Figure 13) by entering two sets of parameters.

It should be pointed out that the purpose of the comparisons in this section is not to examine how closely the model duplicates the details of the example measurements, but rather to show the model's capability of simulating the wide range of key parameter values that arise in actual practice. If simulation values agree (to a given accuracy) with values either pre-chosen or measured, then a quantitative validation of the model can be said to have been achieved. This aspect of validation will be the subject of investigation in future studies.

4. SUMMARY

This report is the third in a series that describes a new approach for modeling the simulation of narrowband or wideband HF propagation channels. The report presents the derivation of and explicit equations for the simulation model transfer function.

The model simulates the time-varying properties of the HF skywave propagation channel and provides a way of studying the effects of different ionospheric conditions on digital communication systems. Besides signal attenuation, the key characteristics that can affect a digital system are:

- (1) time delay spread and amplitude shape factor;
- (2) Doppler frequency shift and spread;
- (3) variation of Doppler frequency with time delay.

These quantities enter as parameters into the simulation model and, through the transfer function, influence and alter the transmitted signal. The manner in which the signal is altered, of course, depends upon the functional form of the transfer function, and this report provides the details of the simulation process.

The report also includes comparisons of the model with NRL measurements from a near-vertical incidence auroral path in Alaska. The model simulates ionospheric conditions ranging from quiet and stable to intense spread-F, and comparisons of scattering functions from model and measurement appear to show good agreement in the primary characteristics. The model is capable of handling multilayer and multimode conditions and, when measurements are available for these kinds of returns, the model provides a convincing representation of the scattering function.

The channel model described here can be used in either a software- or hardware- type simulator, and a hardware HF simulator is currently under development at ITS. This simulator will implement the new model by coupling the transfer function and a newly developed noise/interference model (Lemmon and Behm, 1991) to provide a means of studying the performance of candidate communication systems.

5. ACKNOWLEDGMENTS

The authors wish to thank Dr. D. Bodson and Mr. G. Rekstad of the National Communications System, LTC R. Oldham of the U.S. Army Communications Electronics Command, and Mr. J. Lee of the Department of Defense for their funding support of the work reported in this paper. Thanks are also given to Dr. Len Wagner of the Naval Research Laboratory for permission to use selected plots of measured propagation data for comparison with plots from our model. This work was performed by a United States Government agency and is in the public domain.

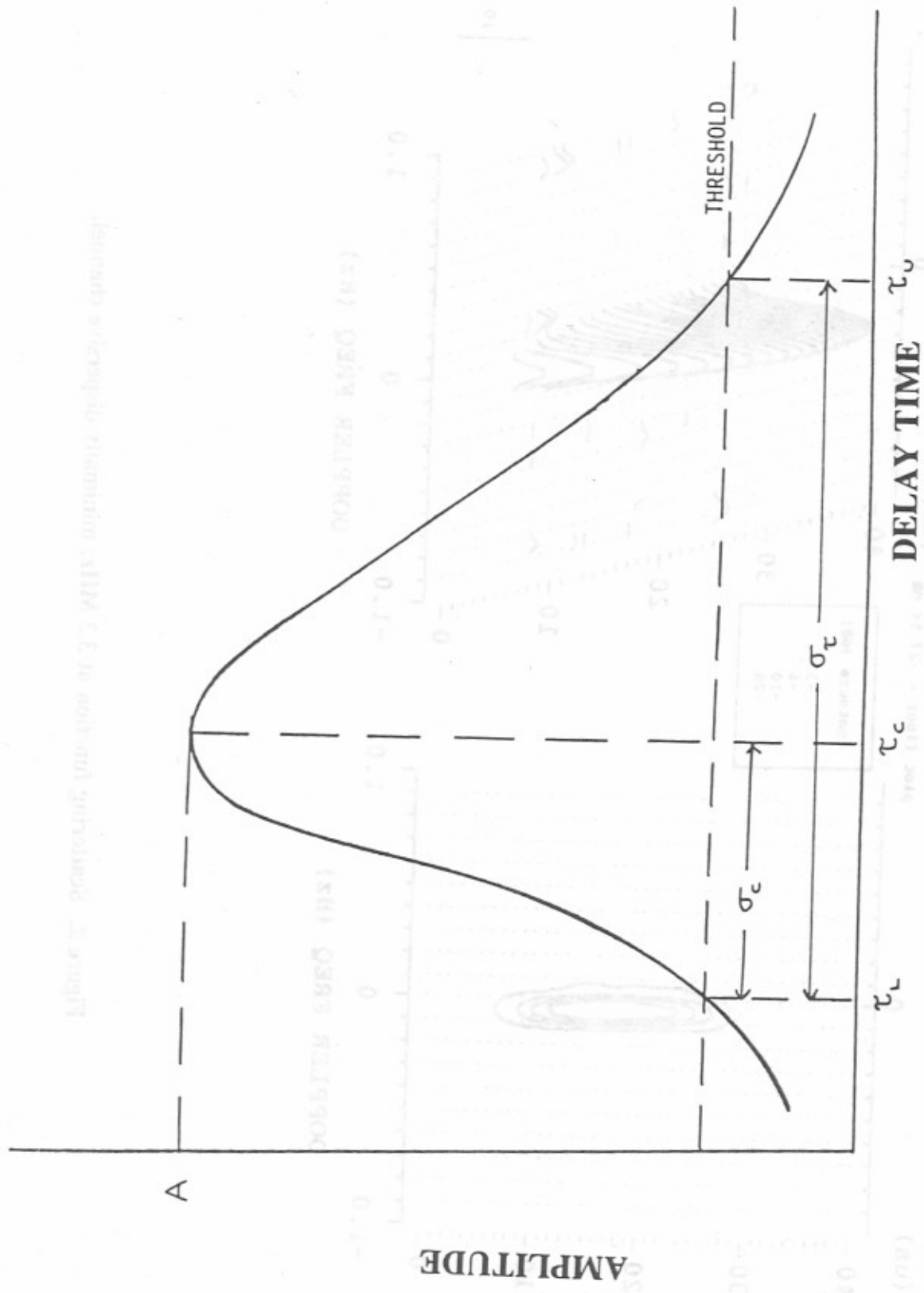


Figure 1. Delay amplitude shape factor.

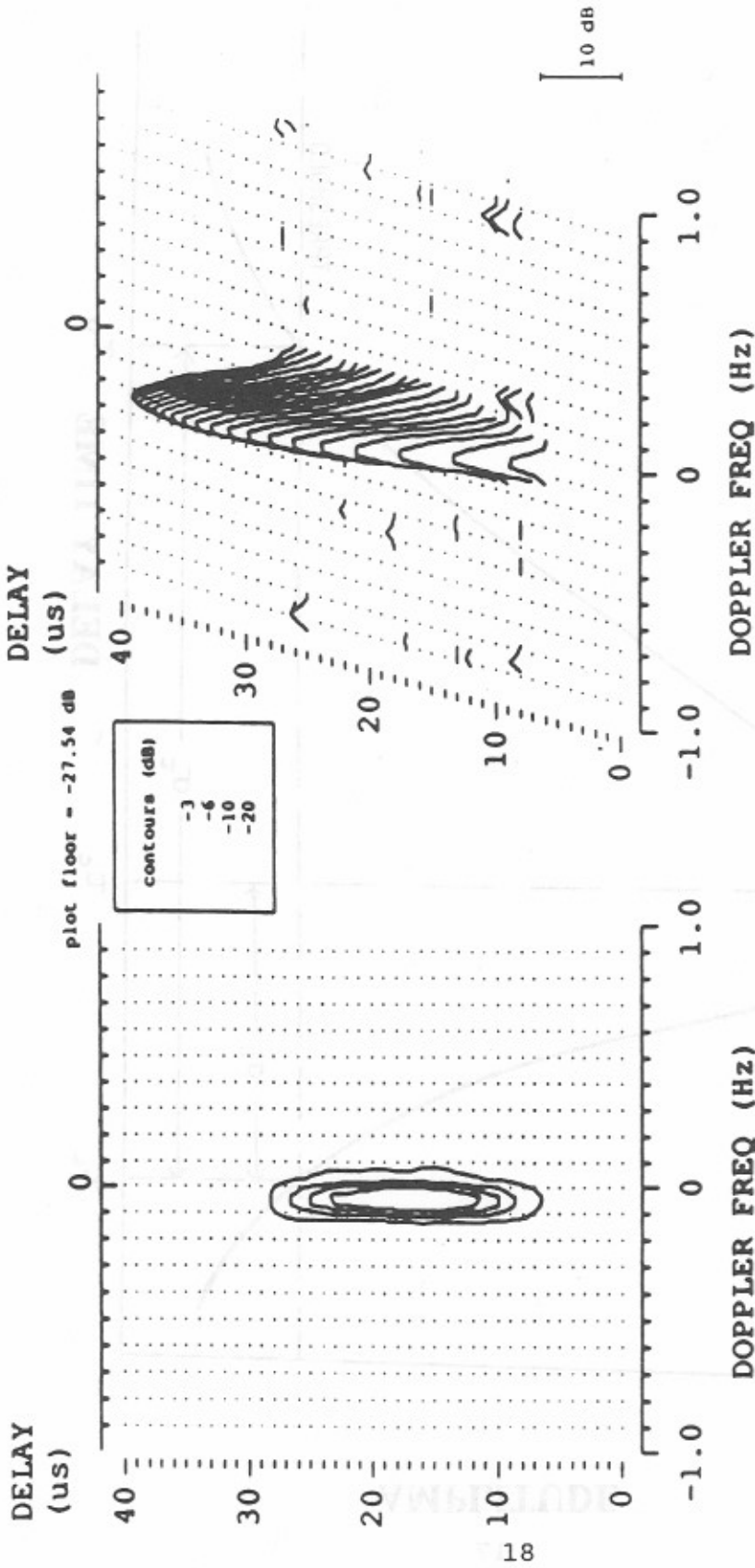


Figure 2. Scattering function at 3.3 MHz; minimally dispersive channel.

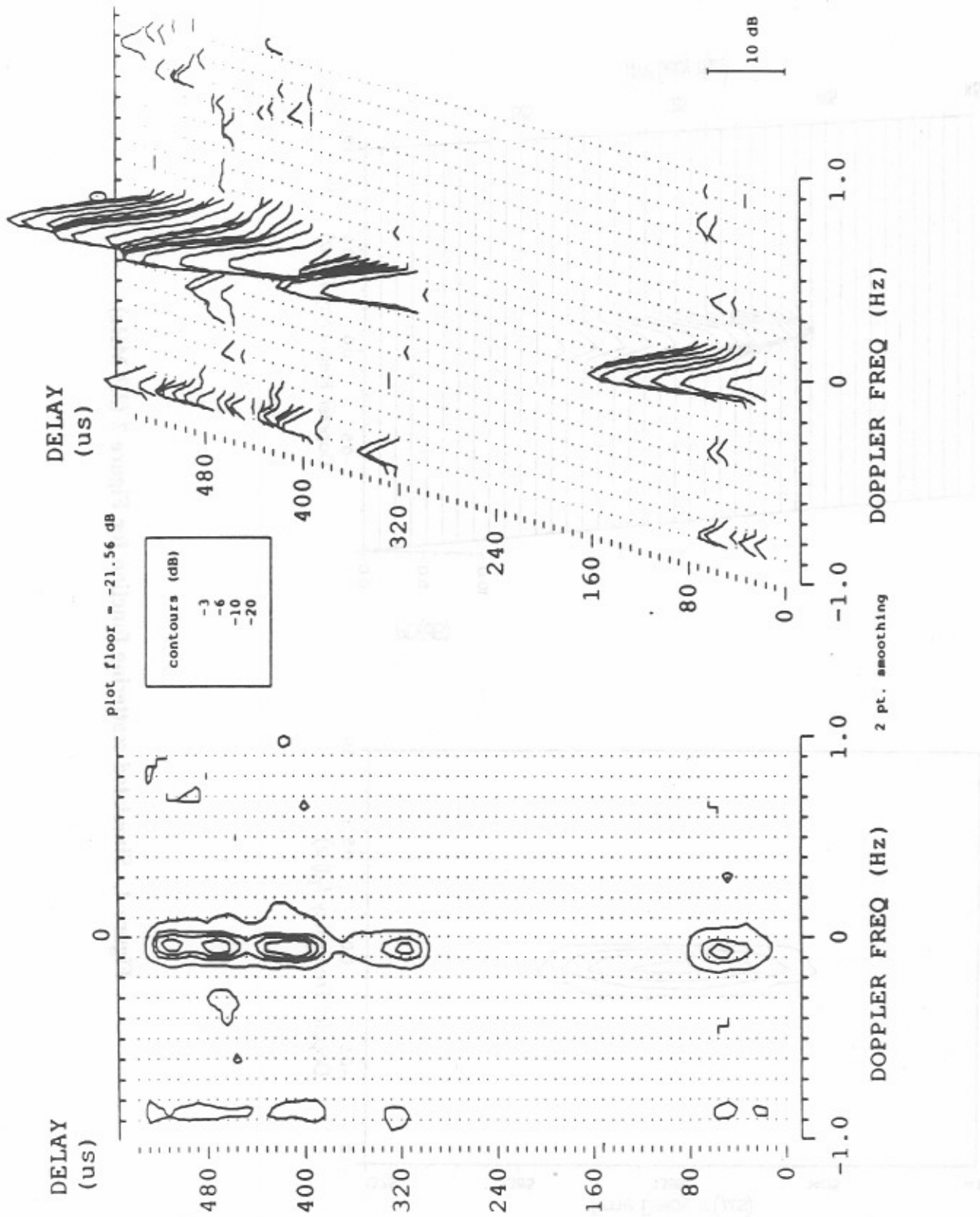


Figure 3. Scattering function at 5.3 MHz; minimally dispersive channel.

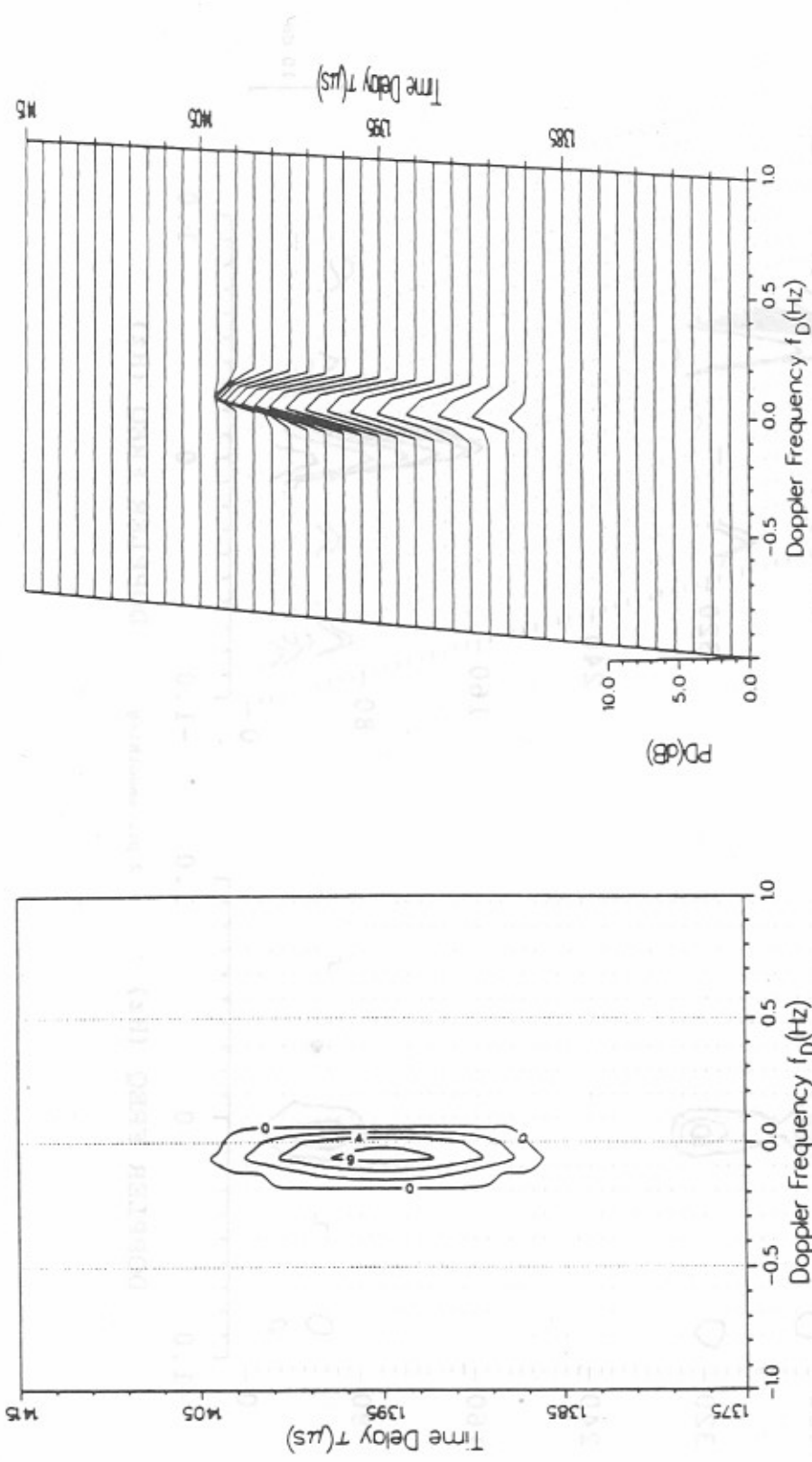


Figure 4. Simulated scattering function for Figure 2 (3.3 MHz).

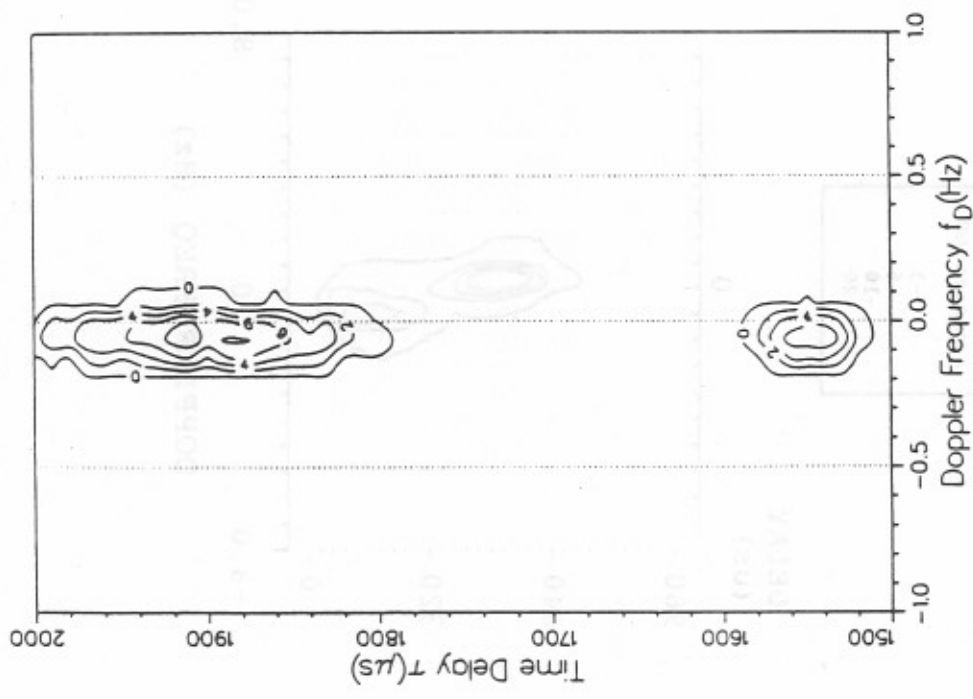
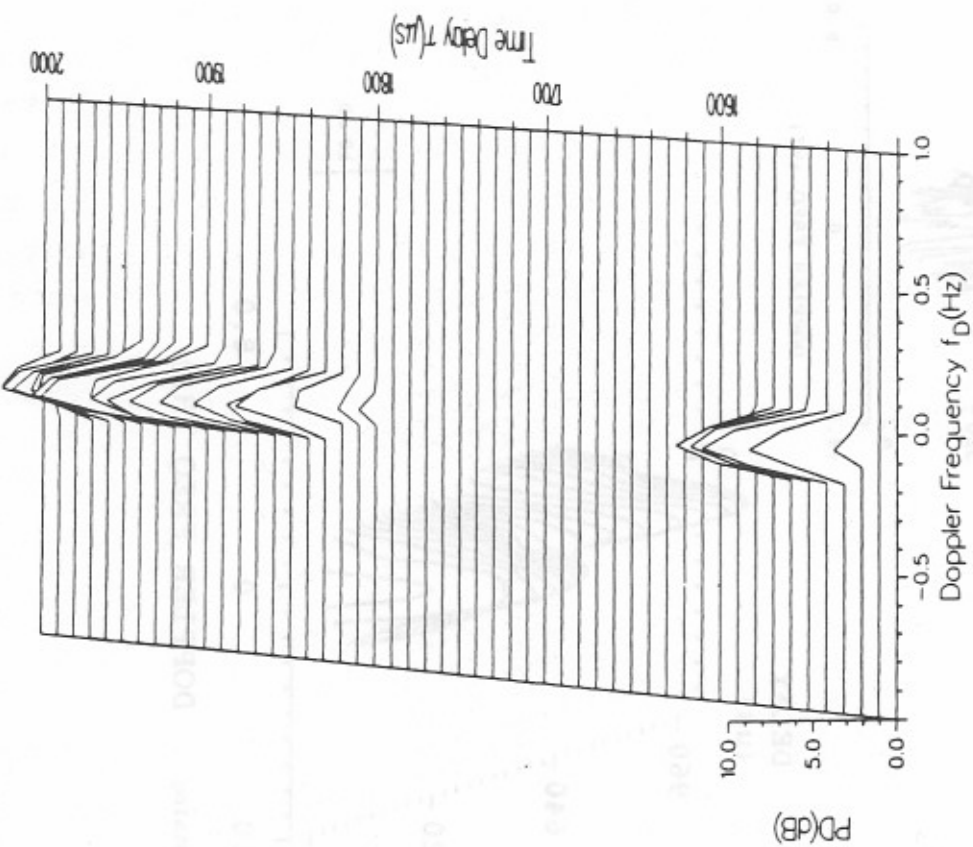


Figure 5. Simulated scattering function for Figure 3 (5.3 MHz).

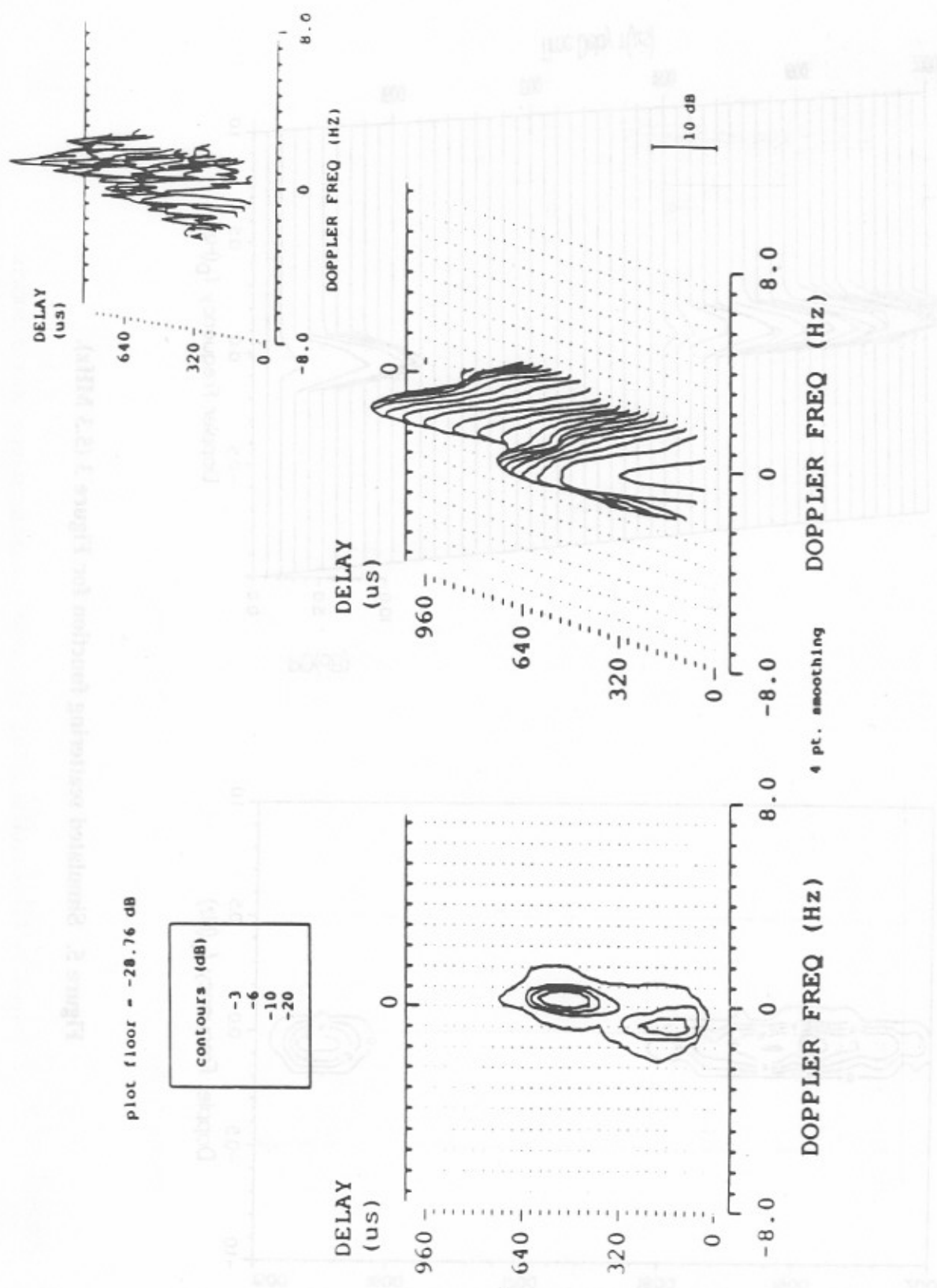


Figure 6. Scattering function at 3.3 MHz; overhead ionospheric trough.

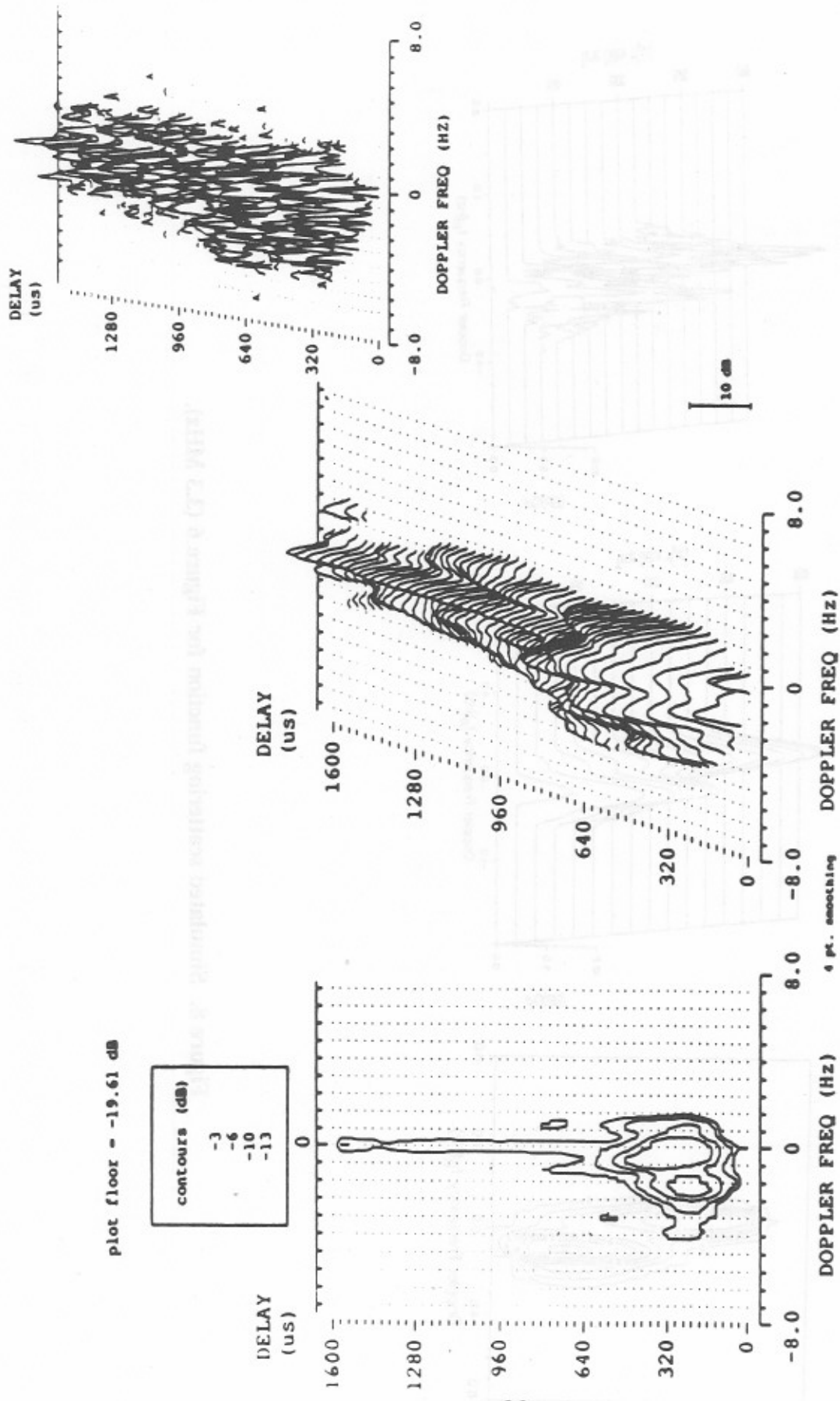


Figure 7. Scattering function at 5.3 MHz; overhead ionospheric trough.

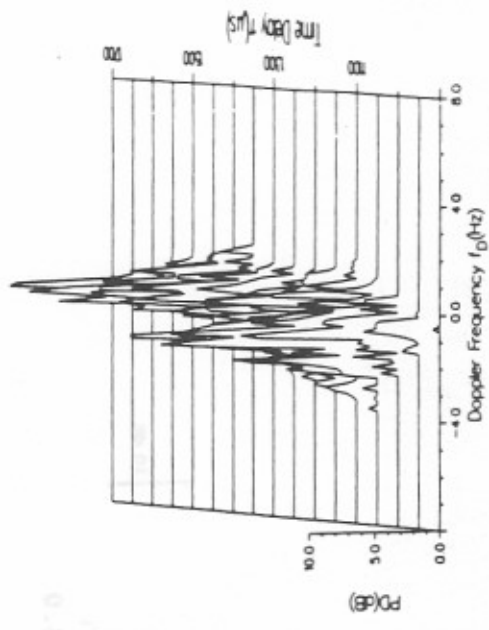
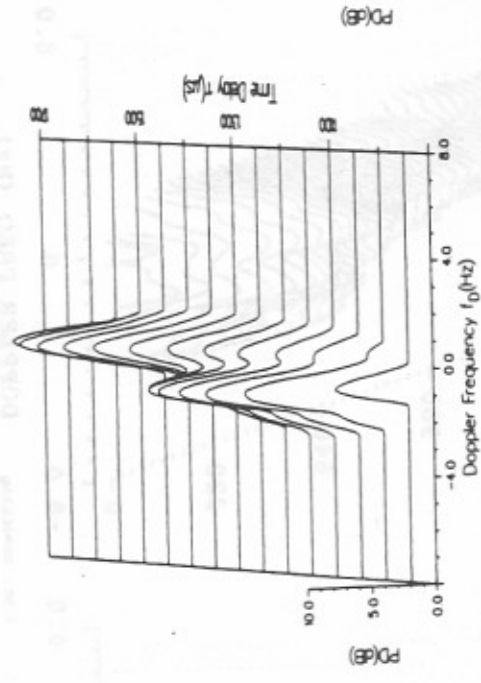
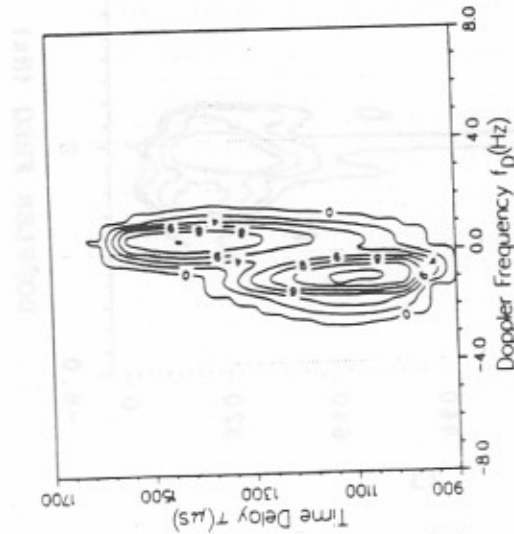


Figure 8. Simulated scattering function for Figure 6 (3.3 MHz).

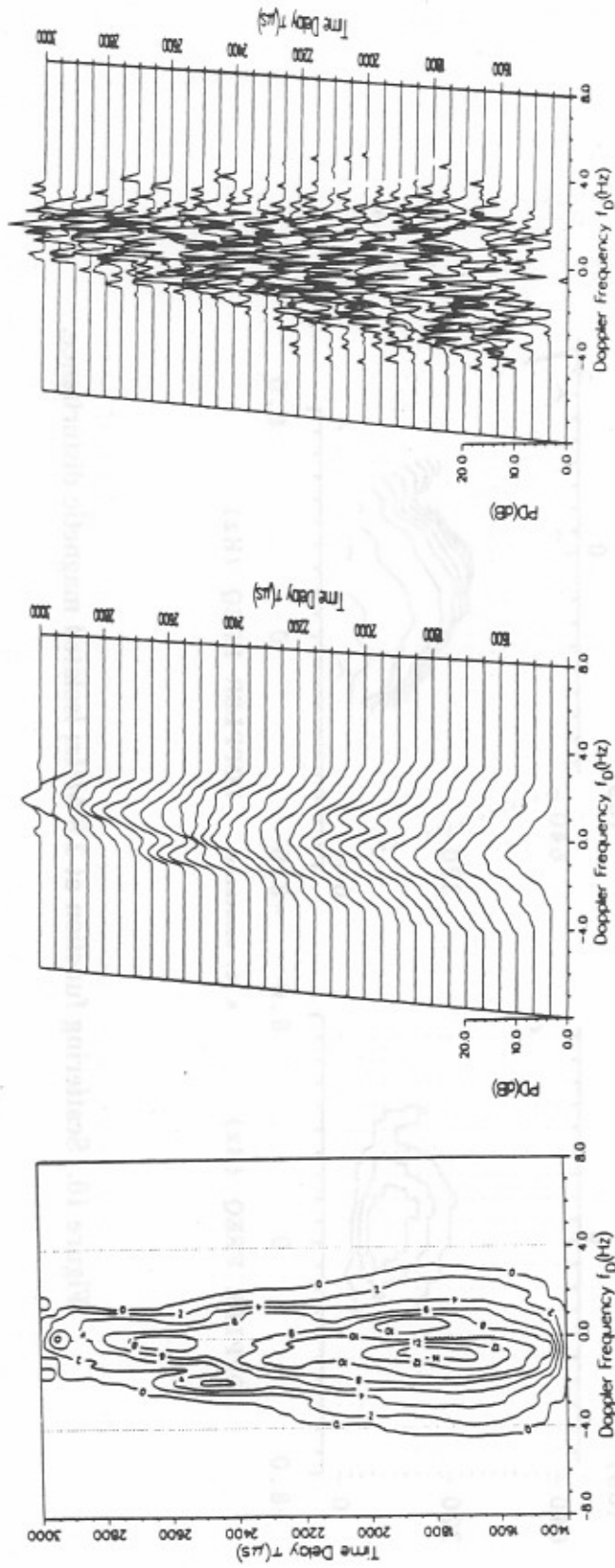


Figure 9. Simulated scattering function for Figure 7 (5.3 MHz).

plot floor = -7.73 dB

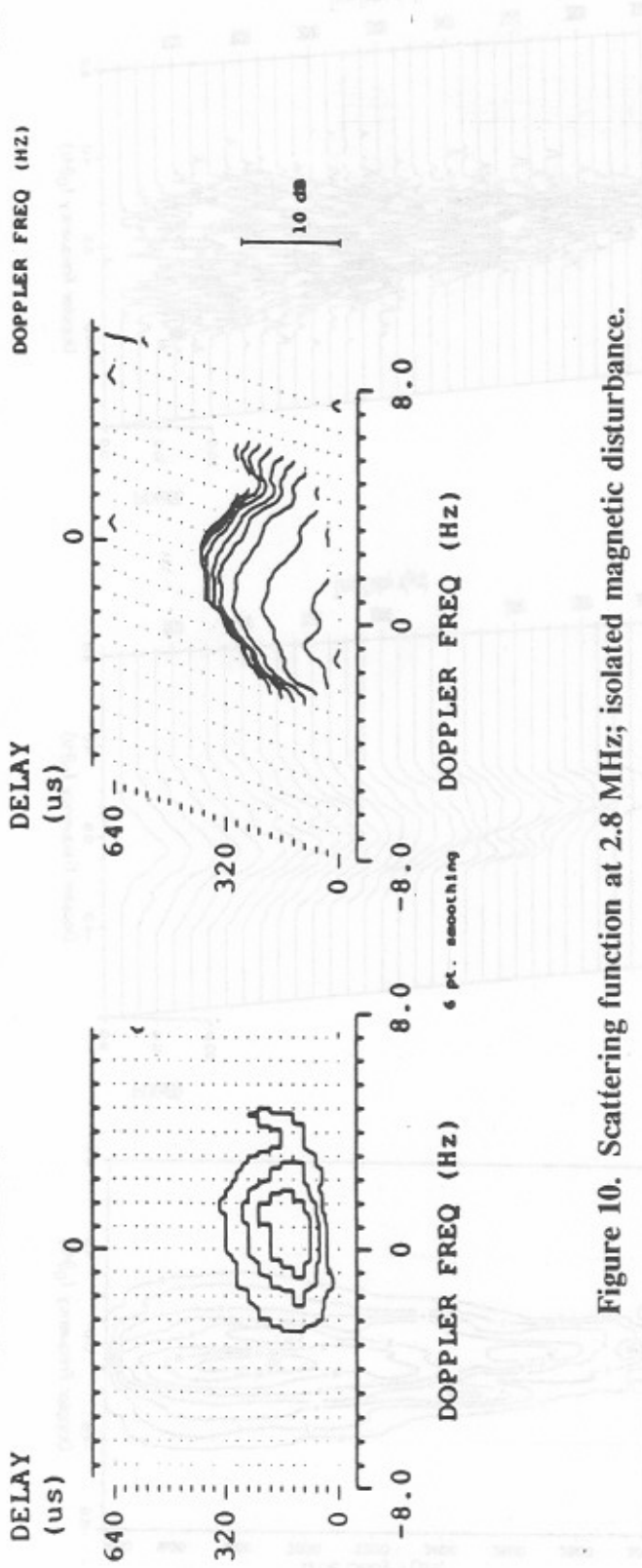
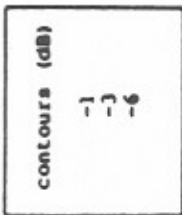


Figure 10. Scattering function at 2.8 MHz; isolated magnetic disturbance.

Figure 11. Scattering function at 3.8 MHz; isolated magnetic disturbance.

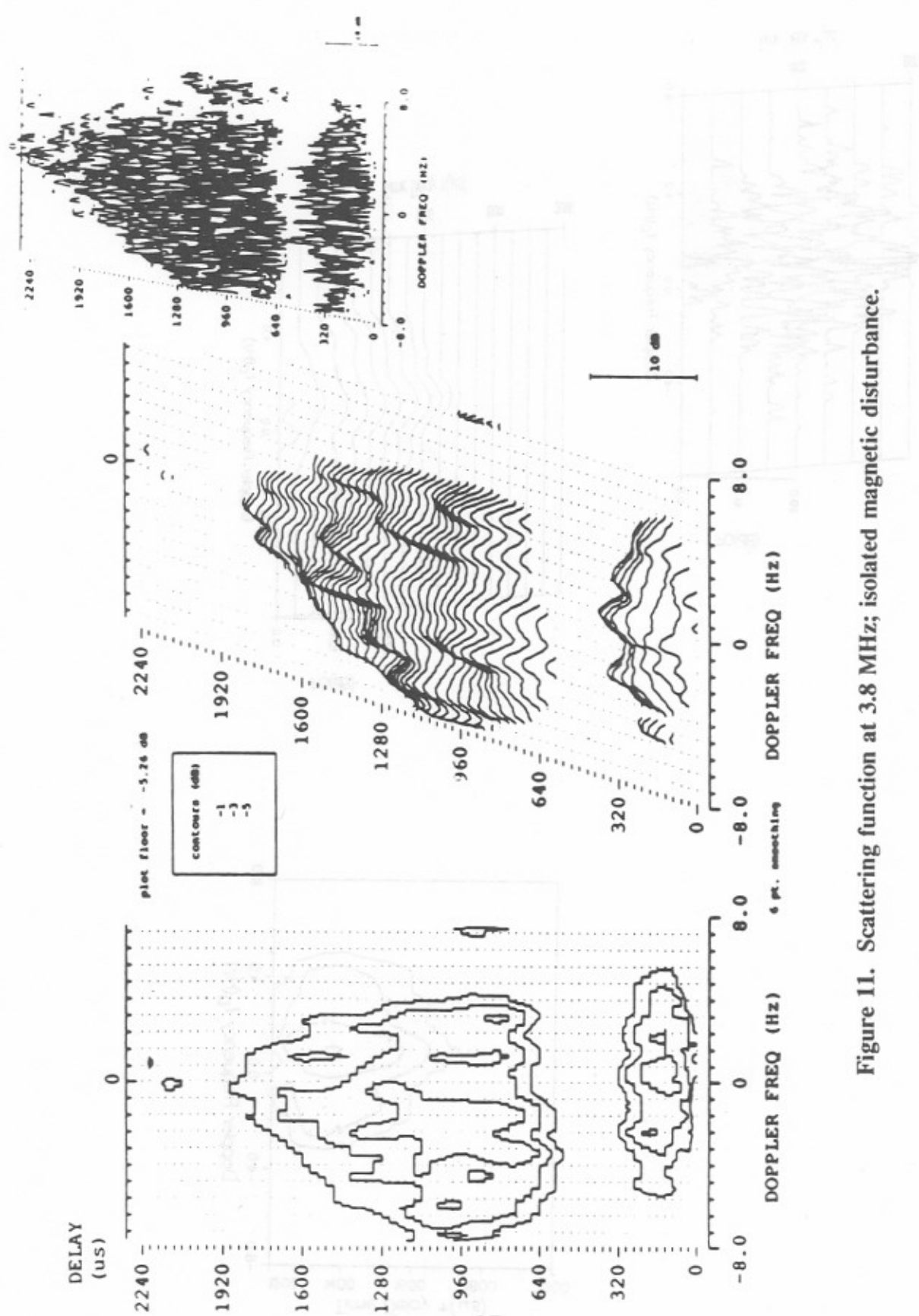


Figure 11. Scattering function at 3.8 MHz; isolated magnetic disturbance.

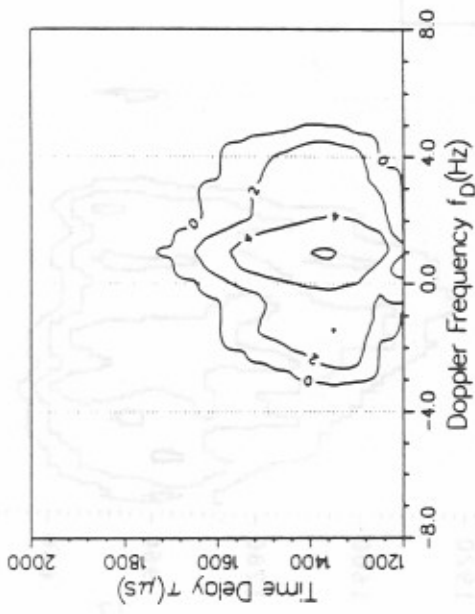
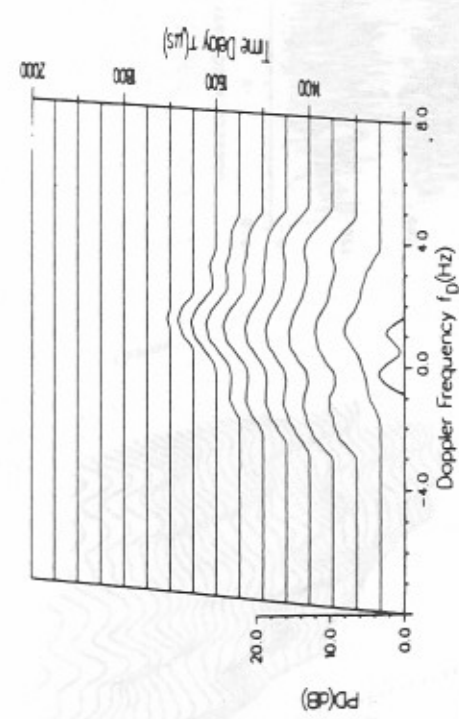
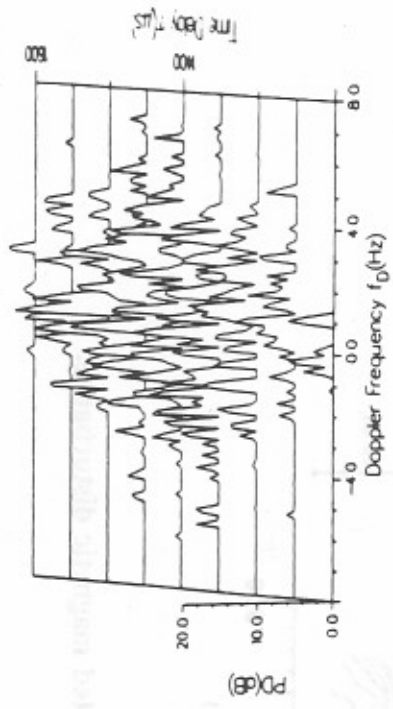


Figure 12. Simulated scattering function for Figure 10 (2.8 MHz).

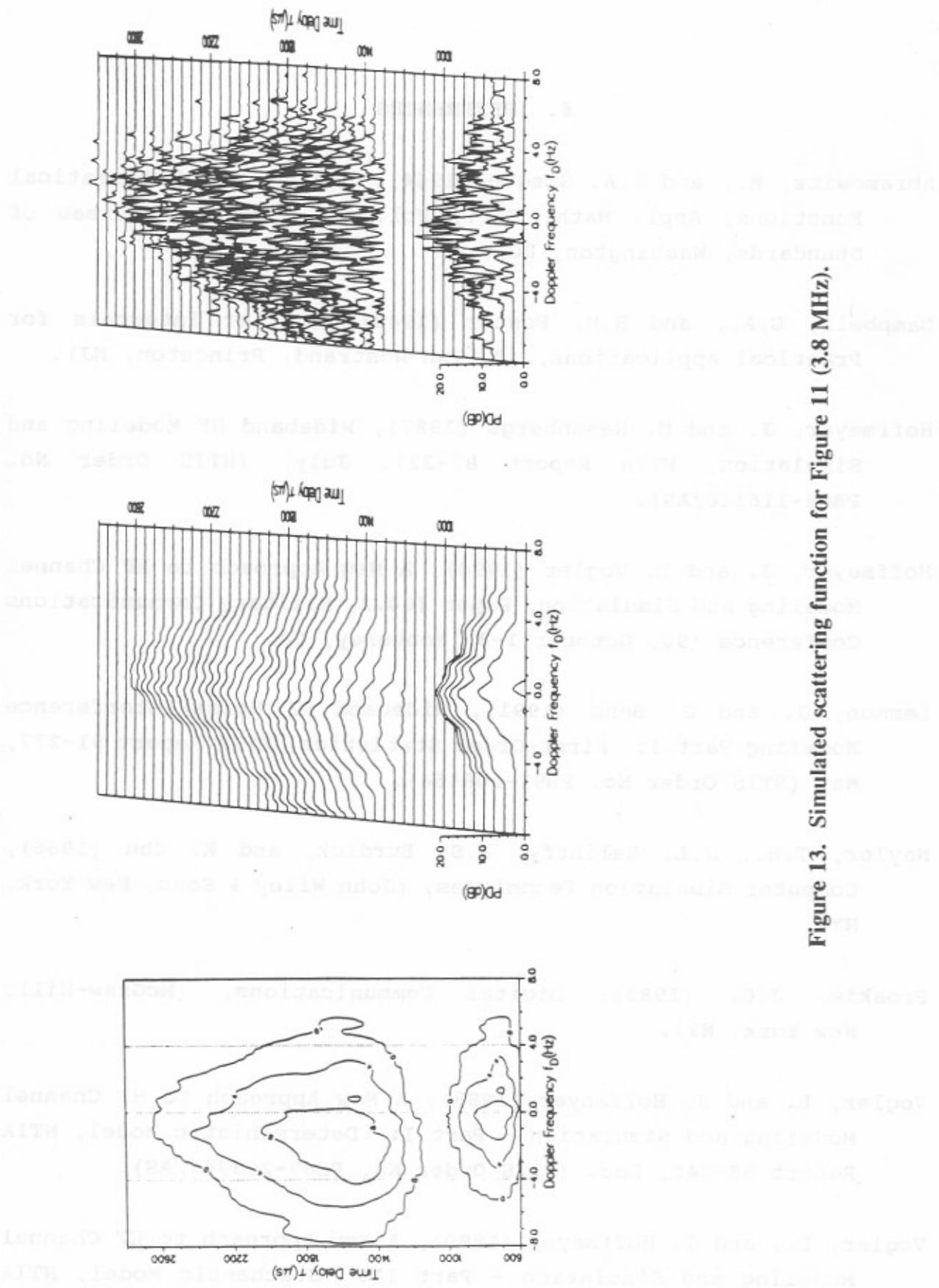


Figure 13. Simulated scattering function for Figure 11 (3.8 MHz).

6. REFERENCES

- Abramowitz, M., and I.A. Stegun (1964), Handbook of Mathematical Functions, Appl. Math. Ser., Vol. 55, (National Bureau of Standards, Washington, DC).
- Campbell, G.A., and R.M. Foster (1948), Fourier Integrals for Practical Applications, (D. Van Nostrand, Princeton, NJ).
- Hoffmeyer, J. and M. Nesenbergs (1987), Wideband HF Modeling and Simulation, NTIA Report 87-221, July, (NTIS Order No. PB88-116116/AS).
- Hoffmeyer, J. and L. Vogler (1990), A New Approach to HF Channel Modeling and Simulation, Paper #60.2, Military Communications Conference '90, October 1-3, Monterey, CA.
- Lemmon, J. and C. Behm (1991), Wideband HF Noise/Interference Modeling Part 1: First-Order Statistics, NTIA Report 91-277, May (NTIS Order No. PB91-208454).
- Naylor, T.H., J.L. Balintfy, D.S. Burdick, and K. Chu (1966), Computer Simulation Techniques, (John Wiley & Sons, New York, NY).
- Proakis, J.G. (1983), Digital Communications, (McGraw-Hill), New York, NY).
- Vogler, L. and J. Hoffmeyer (1988), A New Approach to HF Channel Modeling and Simulation - Part I: Deterministic Model, NTIA Report 88-240, Dec. (NTIS Order No. PB89-203962/AS).
- Vogler, L., and J. Hoffmeyer (1990), A New Approach to HF Channel Modeling and Simulation - Part II: Stochastic Model, NTIA Report 90-255, Feb. (NTIS Order No. PB 90-200338/AS).

6. REFERENCES (cont.)

- Vogler, L., J. Hoffmeyer, J. Lemmon, and M. Nesenbergs (1988), Progress and Remaining Issues in the Development of a Wideband HF Channel Model and Simulator, NATO AGARD Conf. Proc., Propagation Effects and Circuit Performance of Modern Military Radio Systems with Particular Emphasis on Those Employing Bandspreading, Paris, France, Oct. Paper No.6.
- Wagner, L.S., and J.A. Goldstein (1991), Response of the High Latitude HF Skywave Channel to an Isolated Magnetic Disturbance, IEE Conference Publication No. 339, pp. 233-237.
- Wagner, L.S., J.A. Goldstein, W.D. Meyers, and P.A. Bello (1989), The HF Skywave Channel: Measured Scattering Functions for Midlatitude and Auroral Channels and Estimates for Short-Term Wideband HF Rake Modem Performance, MILCOM'89 Conf. Record, Vol. 3, pp. 48.2.1-48.2.10, 1989 IEEE Military Commun. Conf., Boston, Mass.
- Watterson, C.C., J.R. Juroshek, and W.D. Bensema (1970), Experimental Confirmation of an HF Channel Model, IEEE Trans. Commun. Technol. COM-18, pp. 792-803.

Appendix: Derivations for Delay Shape Factor

To determine α and τ_ℓ , the parameters delineating the delay time shape factor, we adapt the following conditions that depend on the overall and the minimum-to-peak delay spreads:

$$\begin{aligned} \ln s_v &= \alpha(\ln z_L + 1 - z_L) = \alpha(\ln z_U + 1 - z_U), \\ \text{where } z_L &= (\tau_L - \tau_\ell) / (\tau_c - \tau_\ell), \quad z_U = (\tau_U - \tau_\ell) / (\tau_c - \tau_\ell), \end{aligned}$$

and $s_v = A_{f\ell}/A$. The delay times τ_L , τ_c , and τ_U are those times associated with, respectively, the lower (minimum), peak, and upper (maximum) τ values of the shape factor; $A_{f\ell}$ denotes the received signal threshold and A is the peak amplitude at τ_c . These conditions lead to the pair of equations

$$\begin{aligned} \ln z_L - z_L &= \ln z_U - z_U, \\ (1 - z_L) / (z_U - 1) &= (\tau_c - \tau_L) / (\tau_U - \tau_c) < 1, \end{aligned}$$

from which z_L may be found from some iterative procedure such as Newton's method. The delay parameters are then given by

$$\begin{aligned} \alpha &= (\ln z_L + 1 - z_L)^{-1} \ln s_v, \\ \tau_\ell &= \tau_c - (\tau_c - \tau_L) / (1 - z_L). \end{aligned}$$

A slight modification of τ_ℓ is made to facilitate the use of the discrete Fourier transform applied later on. The modified τ_ℓ is

$$\tau_{\text{mod}} = [\tau_\ell / \Delta\tau] \Delta\tau,$$

where $[\cdot]$ denotes the nearest integer and $\Delta\tau$ is the delay time increment.

BIBLIOGRAPHIC DATA SHEET

1. PUBLICATION NO. NTIA Report 92-284		2. Gov't Accession No.	3. Recipient's Accession No.
4. TITLE AND SUBTITLE A New Approach to HF Channel Modeling and Simulation Part III: Transfer Function		5. Publication Date March 1992	6. Performing Organization Code NTIA/ITS
7. AUTHOR(S) L.E. Vogler and J.A. Hoffmeyer		9. Project/Task/Work Unit No.	
8. PERFORMING ORGANIZATION NAME AND ADDRESS National Telecommunications & Information Administration Institute for Telecommunication Sciences 325 Broadway Boulder, CO 80303		10. Contract/Grant No.	
11. Sponsoring Organization Name and Address Dept. of the Air Force, Rome Air Development Center Griffiss AFB, NY 13441-5700		12. Type of Report and Period Covered NTIA Report	
14. SUPPLEMENTARY NOTES		13.	
15. ABSTRACT (A 200-word or less factual summary of most significant information. If document includes a significant bibliography or literature survey, mention it here.) This is the third in a series of reports which describe a new and unique approach for modeling either narrowband or wideband high frequency (HF) channels. Although narrowband models of the HF channel have existed for many years, they are applicable to only a limited set of actual narrowband propagation conditions. The need for an HF channel model that is valid for both narrow and wide bandwidths over a more extensive range of propagation conditions motivated the research documented in this series of reports. An explicit expression for the channel transfer function incorporating a random time-varying generator is derived and its relation to the impulse response and scattering function is discussed. Comparisons with measured data indicate the process is best modeled as a sequence of random variables with an exponential autocorrelation function; this leads to a scattering function having a Lorentzian <u>Continued on reverse</u>			
16. Key Words (Alphabetical order, separated by semicolons) channel transfer function; HF channel models; HF propagation; scattering functions; spread spectrum communications; wideband HF			
17. AVAILABILITY STATEMENT <input checked="" type="checkbox"/> UNLIMITED. <input type="checkbox"/> FOR OFFICIAL DISTRIBUTION.		18. Security Class. (This report) Unclassified	20. Number of pages 32
		19. Security Class. (This page) Unclassified	21. Price:

15. ABSTRACT (continued)

shape. A brief discussion of a Gaussian random variable generator is also included. Comparisons of scattering functions from the model and from measurements on a near-vertical incidence auroral path for a wide range of spread-F conditions are shown.